Carbon Dioxide's Liquid−Vapor Coexistence Curve and Critical Properties As Predicted by a Simple Molecular Model

Jonathan G. Harris* and Kwong H. Yung†

Department of Chemical Engineering, Massachusetts Institute of Technology, 25 Ames Street, Room 66-450, Cambridge, Massachusetts 02139

Received: March 14, 1995; In Final Form: May 18, 1995⊗

We present a simple site-based intermolecular potential model for carbon dioxide (the EPM model). It uses point charges and Lennard-Jones interactions centered at each atom. The model predicts a coexistence curve and critical properties quite close to the experimental values. The EPM model predicts a critical temperature of 313.4 ± 0.7 K compared with an experimental critical temperature of 304 K. By rescaling the potential parameters of the EPM model to obtain the model denoted as "EPM2", we more accurately reproduce the liquid−vapor coexistence curve. A flexible EPM model with rigid bonds, but a flexible angle exhibits identical coexistence properties to within the sensitivity of our calculations.

Introduction

Carbon dioxide is a product of many industrial processes, as well as a useful raw material. Recently, many researchers have devoted attention to the possibility of using either liquid or supercritical carbon dioxide as solvents for chemical reactions.[1,2]

The development of accurate physical models for solute solubility and reaction rates in liquid and supercritical carbon dioxide requires a model for intermolecular interactions between carbon dioxide molecules as well as interactions between this solvent and any solutes. Once a model for carbon dioxide has been selected, it is important to characterize it with its predictions of the equation of state, the liquid−vapor coexistence curve, and the critical point properties.

In this work we propose a simple model for carbon dioxide that researchers can readily apply in molecular simulation studies of multicomponent systems. We then locate its critical point for both rigid and flexible versions of the model. This is the first attempt to locate the critical point of any model for CO_2.

Model and Methods

Several earlier workers have proposed models for carbon dioxide.[3−9] Our model has three Lennard-Jones sites with charges centered at each atom. The carbon−oxygen bonds are rigid and 1.163 Å long. This simple model is unique in that it uses point charges centered at atom sites and has a quadrupole moment of 4.3×10^{-26} esu (statcoulomb cm^2 or 4.3 Buckinghams[21]), which is insignificantly different from the experimental value of 4.1×10^{-26} esu.[10] Because it is perhaps the simplest model suitable for simulations of simple mixtures, we refer to it as the elementary physical model (EPM). We examined two variations of this model—a completely rigid object and a model with rigid bond lengths but with a flexible bond angle potential of $^1/_2\, k_\theta(\theta - \theta_0)^2$. Table 1 shows our potential parameters.

In optimizing the Lennard-Jones parameters, we started with those of Murthy, Singer, and McDonald[4] and decreased the oxygen and carbon Lennard-Jones core diameters to get the correct pressure and internal energy at 239 K. We also used point charges that reproduced the gas phase quadrupole moment of 4.3 Buckinghams,[3] instead of the point quadrupole of ref 4.

TABLE 1: Potential Function Parameters for CO_2[a]

EPM Model					
ϵ_{c-c}	28.999 K	σ_{o-o}	3.064 Å	l_{c-o}	1.161 Å
σ_{c-c}	2.785 Å	ϵ_{c-o}	49.060 K	k_θ	1275 kJ/mol/rad^2
ϵ_{o-o}	82.997 K	σ_{c-o}	2.921 Å	q_c	+0.6645 e
EPM2 Model (EPM rescaled to reproduce critical properties)					
ϵ_{c-c}	28.129 K	σ_{o-o}	3.033 Å	l_{c-o}	1.149 Å
σ_{c-c}	2.757 Å	ϵ_{c-o}	47.588 K	k_θ	1236 kJ/mol/rad^2
ϵ_{o-o}	80.507 K	σ_{c-o}	2.892 Å	q_c	+0.6512 e

[a] ϵ and σ are the Lennard-Jones well depth and core diameter in the interatomic potential, $u(r) = 4\epsilon[(\sigma/r)^{12} - (\sigma/r)^6]$. The subscripts refer to the particular atomic pairs interacting. l_{c-o} is the carbon−oxygen bond length, k_θ is the bond bending force constant for the bond stretching potential (for flexible model only), and $u(\theta) = 1/2\, k_\theta\, (\theta - \theta_0)^2$ where θ_0 is 180°. q_c is the charge on the carbon center (positive). There are two equal negative charges on the oxygen centers so that the net charge of the molecule is zero.

References 4 and 7 and others have employed quadrupole moments that are either significantly smaller or larger than the gas phase value. For interactions between unlike atoms, we used the geometric mean combining rule.

We determined the coexistence curve using the Gibbs ensemble technique.[11,12] In this technique there are two noninteracting subsystems. Monte Carlo moves include molecule translations; molecule rotations about a randomly chosen axis in either the x, y, or z direction;[13,14] volume exchanges; and particle exchanges. Volume exchanges involve the uniform dilation of one system and the uniform contraction of the other, keeping the sum of their volumes constant. The acceptance and rejection rules are described in other works.[11,12,15]

For the flexible model, during each rotation attempt we also randomly selected for the trial configuration a new bond angle with unnormalized probability $P(\theta) = \exp(-k_\theta(\theta - \theta_0)^2/(2k_BT))$. Such a procedure meets the detailed balance condition as long as the change in the bond angle energy is not included in the energy change used to determine whether or not to accept the new configuration. This approach is conceptually similar to that of Smit, Karaborni, and Siepmann's treatment of alkanes.[16]

With the exception of the 308 K run, the densities of the coexisting fluids are the average densities in the two subsystems. Because the 308 K run showed large fluctuations, we used the two maxima in the histogram of instantaneous densities in both systems as the values of the mean liquid and vapor densities.

* Author to whom correspondence should be addressed.
† Department of Physics.
⊗ Abstract published in *Advance ACS Abstracts*, July 1, 1995.

0022-3654/95/2099-12021$09.00/0

TABLE 2: Coexistence Properties of Model CO_2[a]

T	$\varrho_{l\,(sim)}$	$\varrho_{l\,(exp)}$	$\varrho_{g\,(sim)}$	$\varrho_{g\,(exp)}$	P (sim)	P (exp)	$\Delta H_{vap\,(sim)}$	$\Delta H_{vap\,(exp)}$	N_{pass}
K	kg/m^3	kg/m^3	kg/m^3	kg/m^3	bar	bar	kJ/mol	kJ/mol	(k)
228	1106(2)	1134.9	19.3(1.2)	21.8	7.6(0.3)	8.2	15.07(0.03)	14.49	40
238	1064(4)	1094.9	23.7(2.0)	31.2	9.5(0.8)	11.9	14.35(0.06)	13.74	6
248	1036(2)	1052.6	37.5(2.2)	43.7	14.9(0.8)	16.6	13.65(0.04)	12.94	40
258	996.9(3)	1006.1	49.4(1.3)	60.2	19.8(0.4)	22.6	12.83(0.03)	12.07	54
268	957.3(3)	956.5	66.8(2.0)	82.4	26.2(0.7)	30.1	11.95(0.03)	10.93	54
278	909.6(3)	898.5	89.6(7.4)	114.7	34.4(1.0)	39.2	10.84(0.03)	9.54	58
288	850.6(4)	824.4	123.2(3)	160.7	45.0(1.1)	50.2	9.50(0.06)	7.81	38
298	777.2(6)	713.0	158.0(4)	241.9	55.2(1.0)	63.5	7.98(0.08)	5.33	81
298[b]	776.0(9)	713.0	164.0(11)	241.9	56.0(1.0)	63.5	7.90(0.05)	5.33	56
303[b]	749.0(5)	593.1	207.5(7)	343.6	63.8(0.5)	71.2	8.28(0.08)	2.72	170
308[b]	680.0(5)		230(2.6)		72.4(0.5)		5.65		142

[a] T is the temperature (Kelvin), ϱ_l and ϱ_g are liquid and gas densities (kg/m^3), respectively, P is the pressure (bar), ΔH_{vap} is the heat of vaporization (kJ/mol), and N_{pass} is the number of passes (thousands) used to generate the property estimates. Quantities labeled (sim) are those computed in this work and those labeled (exp) are experimental measurements reported by Newitt *et al.* in ref 19. [b] Simulation employed 670 molecules instead of 333 molecules. Quantities in parentheses are uncertainties at the 95% confidence level.

We determined the uncertainties (95% confidence) for coexistence densities, pressures, and enthalpies using either the standard deviations of block averages or the method of Dietrich, Scriven, and Davis[17] that employs an integral involving the time correlation function to account for correlations between successive measurements. The block average method employed between 20 and 50 segments.

For the 308 K run we determined the standard deviations of the instantaneous liquid and vapor densities by fitting the density distributions to a sum of two Gaussians. We used the time correlation function to determine the relationship between the standard deviation parameters in the Gaussians and the standard deviation of the mean liquid and vapor densities.

We used the site−site reaction field method with a cutoff distance of 10 Å to treat the Coulomb interactions.[18] The choice of this cutoff likely has some effect upon the phase diagram and should be considered an integral part of the model. Because carbon dioxide has no net dipole moment, the dependence of our results on the truncation scheme should be weaker than that for dipolar molecules such as water. The Lennard-Jones interactions were treated using a spherical cutoff at 10 Å. We included the mean field correction for Lennard-Jones interactions beyond the cutoff in our calculation.

Typical runs involved 333 particles. At 308 K, the 333-particle system spent a significant amount of time at all densities between the maxima in the density histograms corresponding to the liquid and vapor phases. We thus used a 670-particle simulation to obtain properties at this temperature. Typical equilibration times were 2000 passes, although over 20000 passes were needed for equilibration close to the critical point. Ensuring the 308 K state point had reached equilibrium was especially tricky. Each pass involved 1 translation attempt and 1 rotation attempt for each particle, 1 volume change, and 30−300 attempted particle exchanges.

We adjusted the Monte Carlo step sizes to obtain 25−50% acceptance rates for volume exchanges, translations, and rotations. The number of particle exchanges was adjusted to achieve approximately 0.1 (low temperatures) to 1 accepted exchanges per pass. We averaged instantaneous properties over 20 000 to 87 000 passes to obtain the estimates of the macroscopic properties—densities, pressures, chemical potentials, and enthalpies. The conditions of phase equilibria require that the pressures and chemical potentials in the liquid and vapor systems are equal. Our computations are consistent with this requirement; statistical uncertainties can account for any apparent discrepancies. Table 2 includes the number of passes that produced the statistics.

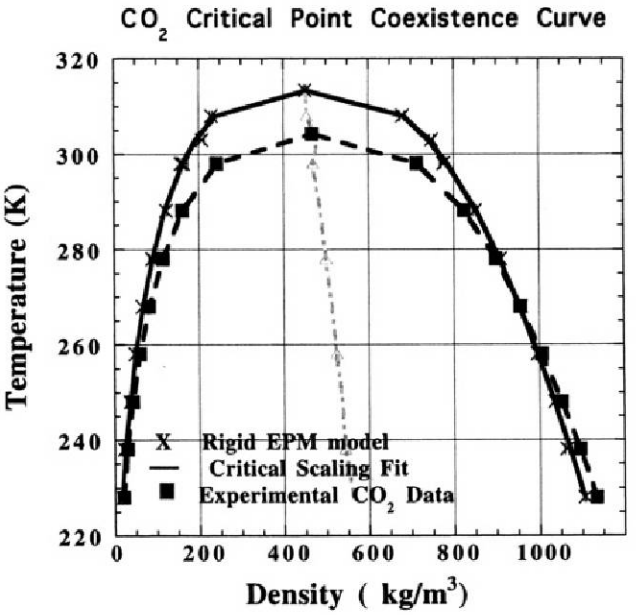

Figure 1. The experimental liquid−vapor coexistence densities of carbon dioxide (filled squares) and those predicted by the EPM model in this work (×). The solid line is the fit to the scaling rules of eqs 1 and 2. The dashed line in the middle with the triangles is the average of the two densities used in the law of rectilinear diameters.

Results

Tables 2 and 3 summarize the coexisting densities, pressures, and heats of vaporization. Figure 1 illustrates the coexistence envelope. We determined the critical temperature, T_c, and the critical exponent, β, by fitting the coexisting densities to the scaling law,

$$(\varrho_l - \varrho_g) = A(T - T_c)^{\beta} \qquad (1)$$

where ϱ_l and ϱ_g are the liquid and vapor densities and A is a proportionality constant determined by the fit.

We used a nonlinear weighted least squares fit. The weights are inversely proportional to the variances of the mean $(\varrho_l - \varrho_g)$. Standard formulas yield standard deviations of the fitting parameters. We estimate the 95% confidence limits of the parameters from their standard deviations using the t-test and use these as our quoted uncertainties. Because the instantaneous densities in the two systems are correlated, we determined the variance of $(\varrho_l - \varrho_g)$ directly from the variances and time correlation functions of the instantaneous difference between the densities of the two systems.

TABLE 3: Coexistence Properties of Model CO_2 with Flexible Bonds[a]

T	$\varrho_{l\,(flex)}$	$\varrho_{l\,(rigid)}$	$\varrho_{g\,(flex)}$	$\varrho_{g\,(rigid)}$	P (flex)	P (rigid)	$\Delta H_{vap\,(flex)}$	$\Delta H_{vap\,(rigid)}$	N_{pass}
K	kg/m^3	kg/m^3	kg/m^3	kg/m^3	bar	bar	kJ/mol	kJ/mol	(k)
258	1001.(2)	996.9	51.7 (1.9)	49.4	20.4(1.7)	19.8	12.81(0.02)	12.83	58
268	952.9(4)	957.3	66.7(3.0)	66.8	26.3(0.5)	26.2	11.91(0.02)	11.95	58
278	905.5(4)	909.6	87.6(5.9)	89.6	33.5(1.6)	34.4	10.84(0.06)	10.84	58
288	854.7(5)	850.6	121.7(6)	123.2	44.3(0.7)	45.0	9.52(0.09)	9.50	60
298	776.0(8)	777.2	160.9(6)	158.0	55.4(0.7)	55.2	7.92 (0.08)	7.98	58

[a] Flex denotes the flexible carbon dioxide model and rigid denotes the rigid model. The units are identical to those of Table 2.

TABLE 4: Experimental Properties vs Properties Predicted from Rescaled Model Using Simulations and Theorom of Corresponding States[a]

T	T_{sim}	$\varrho_{l\,(sim)}$	$\varrho_{l\,(exp)}$	$\varrho_{g(sim)}$	$\varrho_{g(exp)}$	P(sim)	P(exp)	ΔH_{vap} sim	ΔH_{vap} exp
221	228	1140	1162	20	17	7.6	6.3	14.6	15.04
250	258	1028	1047	51	47	20	17.9	12.44	12.73
289	298	801	812	163	165	55	51.4	7.68	7.63

[a] T is the temperature at which the measurements apply. The "sim" results are the predictions for the rescaled EPM described in the Conclusions section, and we obtained them by applying the theorom of corresponding states to the simulations carried out at T_{sim} ($T = 0.97T_{sim}$) for the EPM.

The fit using eq 1 predicts a critical temperature of 313.4 ± 0.7 K [95% confidence limits] and a critical exponent of 0.325 ± 0.009. The critical exponent is statistically indistinguishable from that predicted from renormalization group studies of the three-dimensional Ising model but slightly lower than the experimental critical exponent of 0.355 for the liquid−vapor phase transition.[19]

Because of the smaller data set for the flexible CO_2, we carried out the fit to eq 1 using an exponent fixed at 0.325. Our data predict a critical temperature for the flexible carbon dioxide of 312.8 ± 3 K [95% confidence limit, t-test for 3 degrees of freedom], which is indistinguishable from that from the rigid model. The critical temperature is about 3% higher than the experimentally measured value for carbon dioxide of 304.2 K.[20]

Because eq 1 is an asymptotic equation which loses accuracy as one moves away from the critical point, our fitting procedure could produce some bias. We applied this procedure to the experimentally determined coexistence curve of carbon dioxide. Fitting data from 228 to 298 K underestimates the critical temperature by 1.1 K and produces a critical exponent of 0.325 instead of 0.355, the correct value. Using only the experimental points from 268 to 298 K would still understate the critical by 0.7 K and predict a critical exponent of 0.333. Using only our higher temperature data to estimate the critical point from the simulations is not practical because of the statistical uncertainties. Fitting the experimental data in the range of temperatures T = 248 to 288 while fixing the exponent to 0.325 (which corresponds to the situation used with the flexible model) predicts a critical temperature which is also 1 K too low (allowing a variable exponent lowers the fitted critical temperature by another degree K).

We expect the finite size effects on the predicted critical point to be small at our system sizes. For the 298 K system, Table 2 compares two system sizes—333 molecules and 670 molecules. The predictions are identical to within the statistical uncertainties. Predictions for lower temperatures should exhibit even smaller finite size effects because of smaller correlation lengths. Thus, for the location of the critical point, we would expect the finite size effects to be comparable to the statistical uncertainties.

We determined the critical density by a similar fit to the law of rectilinear diameters,

$$1/2\,(\varrho_l + \varrho_g) = \varrho_c + A(T - T_c) \qquad (2)$$

The critical density of the rigid and flexible models are 453.7 ± 4.3 kg/m^3 and 449 ± 16 kg/m^3. The experimental critical density of carbon dioxide is slightly higher, 468.0 kg/m^3.[20]

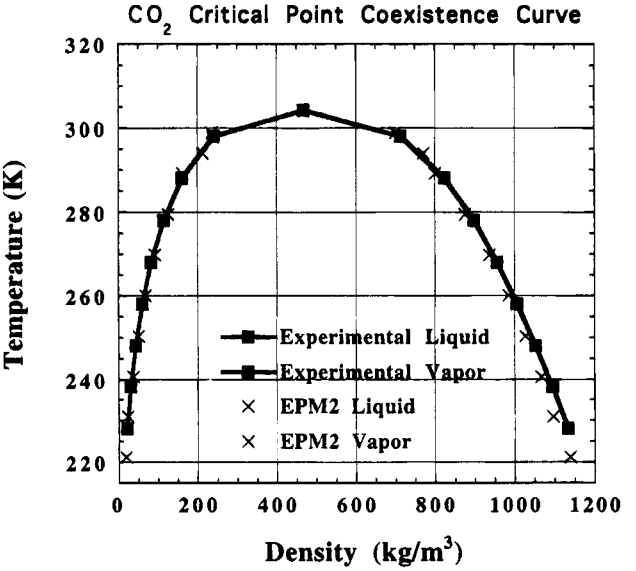

Figure 2. The experimental liquid−vapor coexistence densities of carbon dioxide (filled squares) and those predicted by the EPM2 (rescaled) model (×).

We determined the critical pressure of the rigid model by carrying out a constant N−V−T Monte Carlo simulation at densities of 305 and 597 kg/m^3 and $T = T_c$ = 313.4 K. Because the critical density predicted from the law of rectilinear diameters is the mean of these two densities, the critical pressure is the mean of the two pressures, 73.4 ± 6.4 and 79.7 ± 0.9, according to the critical scaling laws.[21] We thus predict a critical pressure of 76.5 ± 4.5 bar. This is within the statistical uncertainty of experimental critical pressure of 73 bar.

Conclusions

The EPM model with the parameters in Table 1 predicts values of the critical properties that are in agreement with the available experimental data. Its critical point is only 3% too high, and its critical density is 3% too low.

Using the theorem of corresponding states, we can obtain nearly exact agreement between the experimental and theoretical critical properties by multipling the Lennard-Jones well depths, the length parameters (bond lengths and Lennard-Jones core sizes), and charges by 0.9700, 0.9900, and 0.9800, respectively. Such a model we denote as "EPM2". Table 1 shows the

appropriate parameters for the EPM2 model . Figure 2 and Table 4 show the comparison between its coexistence curve and the experimental one. Although such a model predicts the critical point accurately, it consistently underpredicts the liquid coexistence densities by 1−2% at temperatures between 221 and 289 K.

Acknowledgment. This work was funded by the Emissions Reduction Research Center (ERRC) and the Petroleum Research Fund. Some of the computations were carried out on the Cray C-90 at the Pittsburgh Supercomputer Center. We thank Dr. Shengting Cui for his advice.

References and Notes

(1) Ikushima, Y.; Saito, N.; Arai, M. *J. Phys. Chem.* **1992**, *96*, 2293−2297.

(2) Roberts, C. B.; Chateauneuf, J. E.; Brennecke, J. F. *J. Am. Chem. Soc.* **1992**, *114*, 8455−8463.

(3) Etters, R. D.; Kuchta, B. *J. Chem. Phys.* **1989**, *90*, 4537−4541.

(4) Murthy, C. S.; Singer, K.; McDonald, I. R. *Mol. Phys.* **1981**, *44*, 135−143.

(5) Geiger, L. C.; Ladanyi, B. M.; Chapin, M. E. *J. Chem. Phys.* **1990**, *93*, 4533−4542.

(6) Palmer, B. J.; Garrett, B. C. *J. Chem. Phys.* **1993**, *98*, 4047−4058.

(7) Zhu, S. B.; Robinson, G. W. *Comput. Phys. Commun.* **1989**, *52*, 317−321.

(8) Gibbons, T. G.; Klein, M. L. *J. Chem. Phys.* **1974**, *60*, 112−126.

(9) Böhm, H. J.; Ahlrichs, R.; Scharf, P.; Schiffer, H. *J. Chem. Phys.* **1984**, *81*, 1389−1395.

(10) Buckingham, A. D.; Disch, R. L. *Proc. R. Soc. A.* **1963**, *273*, 275−289.

(11) Panagiotopoulos, A. Z. *Mol. Simul,* **1992**, *9*, 1−24.

(12) Panagiotopoulos, A. Z. *Mol. Phys.* **1987**, *61*, 813−826.

(13) Barker, J. A.; Watts, R. O. *Chem. Phys. Lett.* **1969**, *3*, 144−145.

(14) Allen, M. P.; Tildesley, D. J. *Computer Simulation of Liquids*; Clarendon Press: Oxford, 1990.

(15) Smit, B.; Smedt, P. D.; Frenkel, D. *Mol. Phys.* **1989**, *68*, 931−950.

(16) Smit, B. ; Karaborni, S.; Siepmann, J. I. *J. Chem. Phys.* **1995**, *102*, 2126−2140.

(17) Deitrick, G. L.; Davis, H. T.; Scriven, L. E. *J. Chem. Phys.* **1989**, *90*, 2370.

(18) Hummer, G.; Soumpasis, D. M.; Neumann, M. *Mol. Phys.* **1992**, *77*, 769−785.

(19) Hansen, J. P.; McDonald, I. R. *Theory of Simple Liquids*, 2nd ed.; Academic Press: Boston, 1986.

(20) Newitt, D. M.; Pai, M. U.; Kuloor, N. R.; Huggill, J. A. W. In *Thermodynamic Functions of Gases*; Din, F. Ed.; Butterworth: London, 1956; Vol. 123.

(21) Hansen, J. P.; McDonald, I. R. *Theory of Simple Liquids*, 1st ed.; Academic Press: New York, 1976.

JP9507197